Electronic supplementary information

Engineering surface defects-rich Ti_3C_2 quantum dots/mesoporous C_3N_4 hollow nanosphere Schottky junction for efficient N_2 photofixation

Binbin Chang,[a] Yanzhen Guo,[b] Huili Liu,[b] Li Li,*[a] and Baocheng Yang*[b]

[a]Shanghai Key Laboratory of Green Chemistry and Chemical Processes, School of Chemistry and Molecular Engineering, East China Normal University, Shanghai 200241, China

[b]Henan Provincial Key Laboratory of Nanocomposites and Applications, Institute of Nanostructured Functional Materials, Huanghe Science and Technology College, Zhengzhou 450006, China

Apparent quantum efficiency measurements

For the measurement of the apparent quantum efficiencies (AQEs), the N_2 photofixation reactions were performed under monochromatic light using appropriate bandpass filters at different wavelengths (380, 420, 475, 520, 550, 600, 650 and 700 nm, full widths at half maximum for all: 20 nm, Beijing MerryChange Technology). The corresponding power intensities were measured using an optical power meter (Molectron POWER MAX 5200). The AQEs under different monochromatic light were calculated according to the following equation

$$AQE\ (\%) = \frac{N_{\text{reacted}}}{N_{\text{incident}}} \times 100\% = \frac{3N_{NH_3}}{N_{\text{incident}}} \times 100\% = \frac{3n_{\text{NH}_3} \times N_{\text{A}}}{(W \times A \times t)/(hv)} \times 100\%$$

where N_{reacted}, N_{incident} and N_{NH_3} represent the numbers of the reacted electrons, the incident photons and the generated NH_3 molecules, respectively, W, A and t respectively denote the light intensity, illumination area and illumination time, v is the light frequency, h is Planck's constant, and N_{A} is Avogadro's constant.

Solar-to-ammonia conversion efficiency measurements

To determine the solar-to-ammonia (STA) conversion efficiency, the photocatalytic N_2 fixation reactions were carried out in a sealed reactor under simulated AM1.5G light illumination. Typically, 200 mg of the photocatalyst and 50 mL of water were added into the reactor. The reaction system was vacuumed and blown with N_2 repeatedly several times to drive out the dissolved air completely and then sealed with a rubber plug. To make sure that the reaction system was filled with N_2, it was further bubbled for another 1 h with a N_2-filled balloon. After the reaction solution was subjected under the simulated AM1.5G light illumination for 1 h, the produced ammonia amount was determined using Nessler's method. In addition, the evolved gases were also measured on a gas chromatograph (CEAULIGHT GC-7900, TCD detector, Ar carrier gas). The photocatalytic reaction was repeated three times.

The STA efficiency was calculated based on the equation below

$$\text{STA efficiency} = \frac{\left[\Delta G^0 \; for \; NH_3 \; generation \; (J \; mol^{-1})\right] \times [evolved \; NH_3 \; (mol)]}{[total \; input \; light \; power \; (W)] \; \times [reaction \; time \; (s)]} \quad (3)$$

Similarly, the solar-to-hydrogen (STH) efficiency can be calculated as

$$\text{STH efficiency} = \frac{\left[\Delta G^0 \; for \; H_2 \; generation \; (J \; mol^{-1})\right] \times [evolved \; H_2 \; (mol)]}{[total \; input \; light \; power \; (W)] \; \times [reaction \; time \; (s)]}$$

In the above equation, the ΔG^0 value for NH_3 and H_2 generation are 339 and 237 kJ mol^{-1}. The overall illumination intensity of the AM 1.5G light source was 100 mW cm^{-2} and the illumination area is 23.75 cm^2.

Electrochemical measurements

To prepare the working electrode, the catalyst was first dispersed in an ethanolic solution of Nafion (5.0 vol%) to form an ink (10 mg mL^{-1}). The resultant dispersion (0.2 mL) was then dip-coated onto an indium tin oxide (ITO)-coated glass electrode with a coated area of 1 cm^2 and allowed to dry in a vacuum oven overnight at room temperature. The photocurrent and electrochemical impedance spectroscopy (EIS) measurements were conducted on an electrochemical workstation (CHI 760E, Shanghai Chenhua) in a three-electrode system with an electrolyte solution of 0.5 M Na_2SO_4, using Pt foil as the counter electrode, the standard Ag/AgCl electrode as the reference electrode, and the ITO substrate as the working electrode. All measurements were carried out at room temperature in Na_2SO_4 aqueous solution that has been

deoxygenated by bubbling high-purity Ar for 30 min. Photocurrent measurements were performed at a potential of 0.2 V (*vs*. Ag/AgCl) under visible light irradiation (300 mW/cm^2).

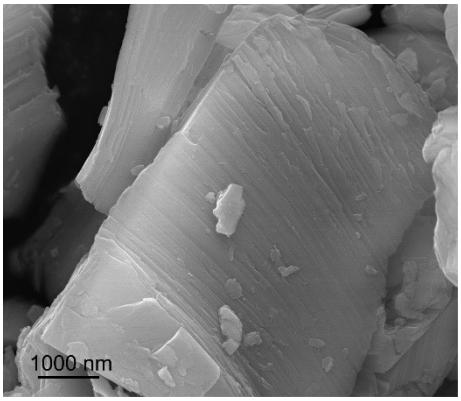

Fig. S1 SEM image of Ti_3AlC_2.

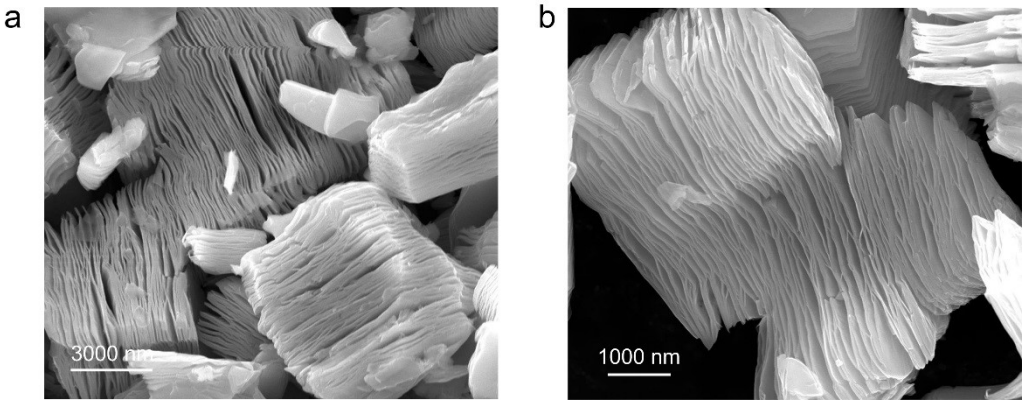

Fig. S2 SEM images of Ti_3C_2 MXene. (a) Low magnification. (b) High magnification.

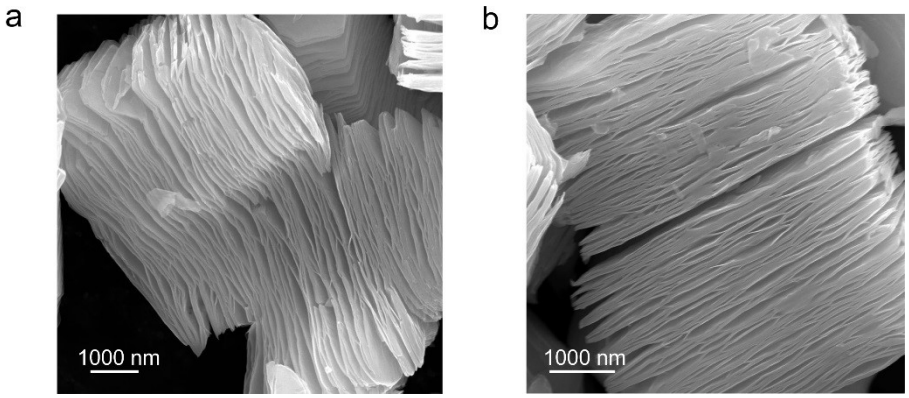

Fig. S3 SEM images of r-Ti_3C_2 MXene.

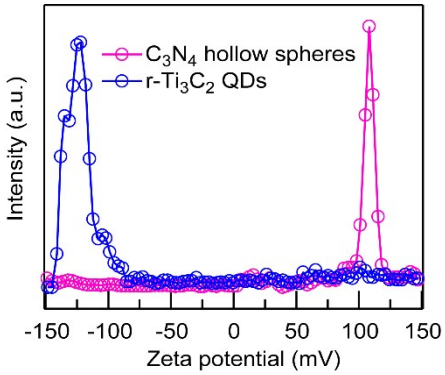

Fig. S4 Zeta potential measurements. The Zeta potentials of C_3N_4 hollow spheres and r-Ti_3C_2 QDs.

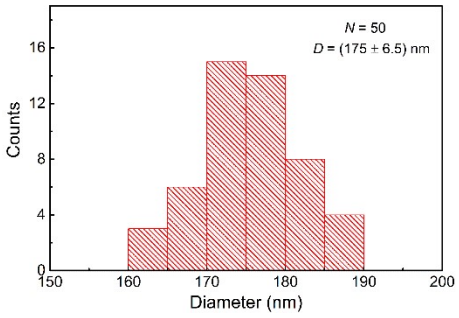

Fig. S5 Histogram of the diameter distribution of solid silica spheres

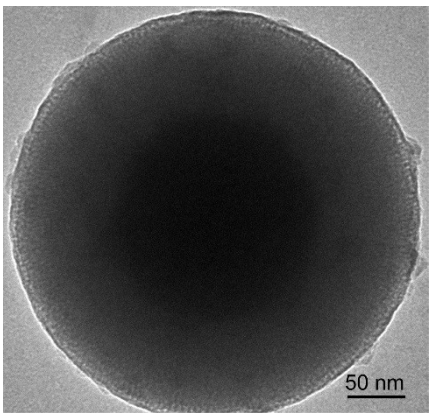

Fig. S6 The high-magnification TEM image of SiO_2@mSiO_2.

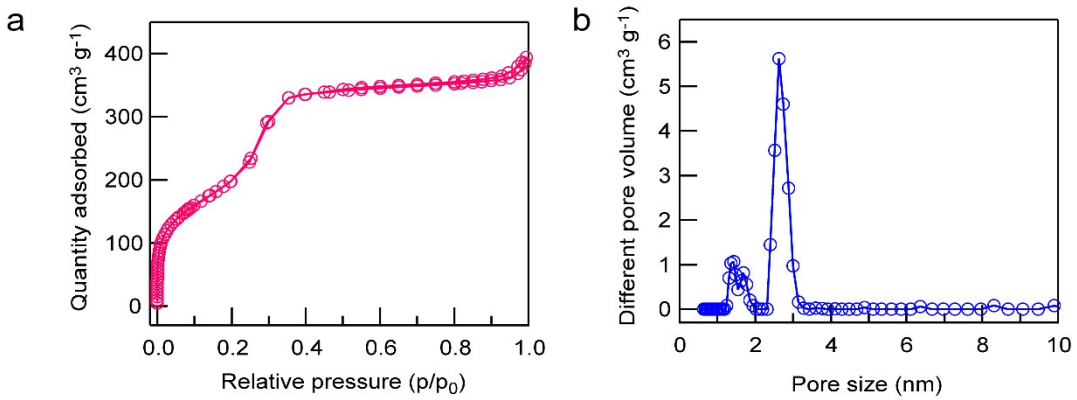

Fig. S7 (a)The N_2 adsorption-desorption isotherm of SiO_2@mSiO_2 and (b) pore size distribution of SiO_2@mSiO_2.

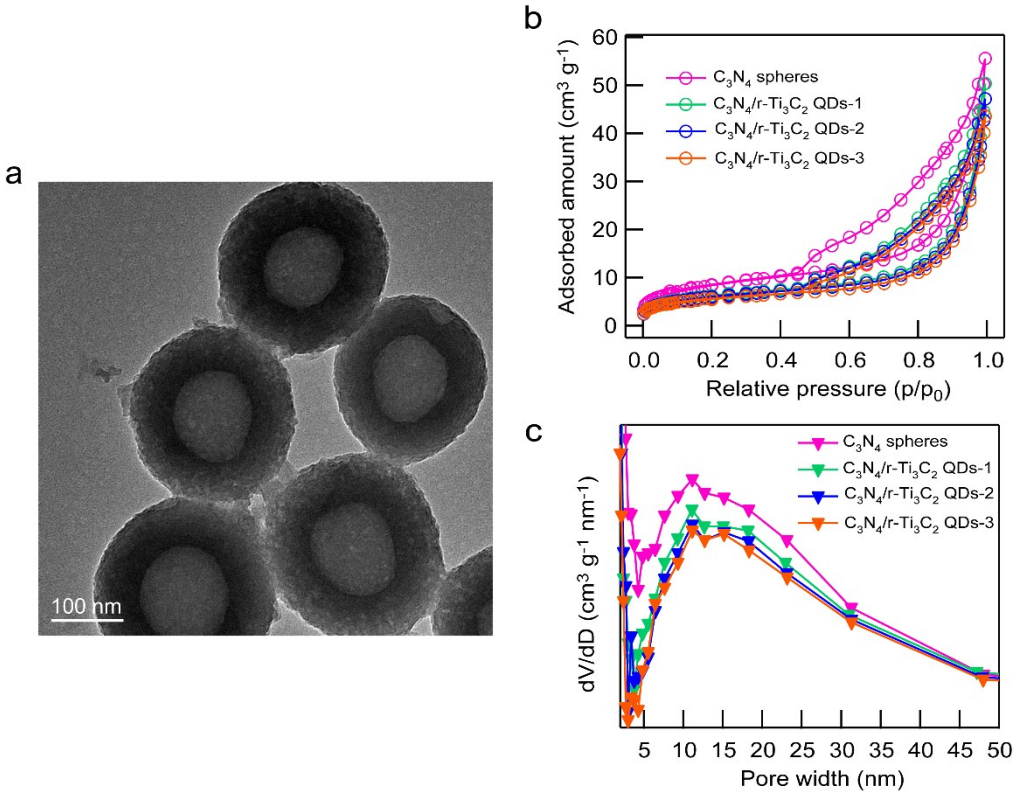

Fig. S8 (a) The high-magnification TEM image of C_3N_4 hollow spheres. (b) The N_2 adsorption-desorption isotherms of C_3N_4 hollow spheres and C_3N_4/r-Ti_3C_2 QDs. (c) The pore size distribution of C_3N_4 hollow spheres and C_3N_4/r-Ti_3C_2 QDs.

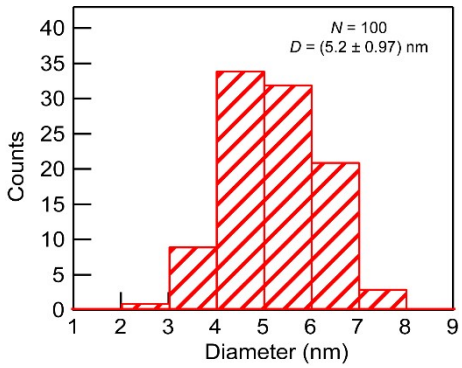

Fig. S9 Histogram of the diameter distribution of r-Ti_3C_2 QDs.

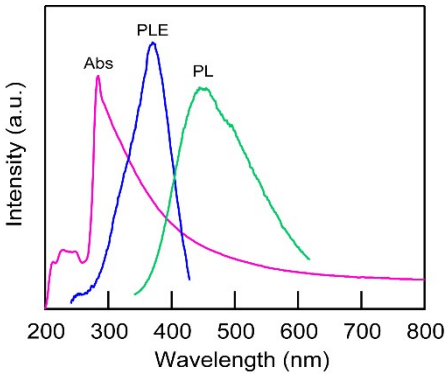

Fig. S10 UV-vis absorbance, the maximum excitation and emission spectra of the r-Ti_3C_2 QDs

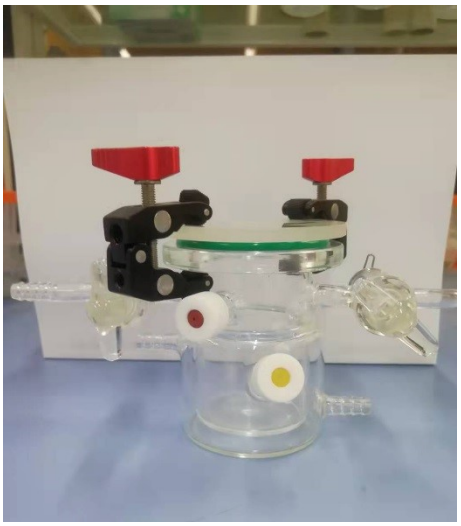

Fig. S11 Photograph of the photocatalytic N_2 fixation reactor.

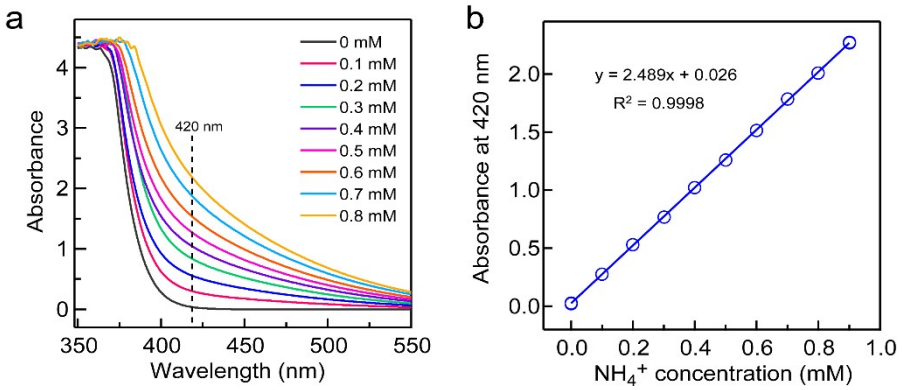

Fig. S12 Dependence of the absorbance on the NH_4^+ determination. (a) Absorption spectra of the standard NH_4^+ solutions at different concentrations. (b) Linear relationship between the absorbance at 420 nm and the NH_4^+ concentration.

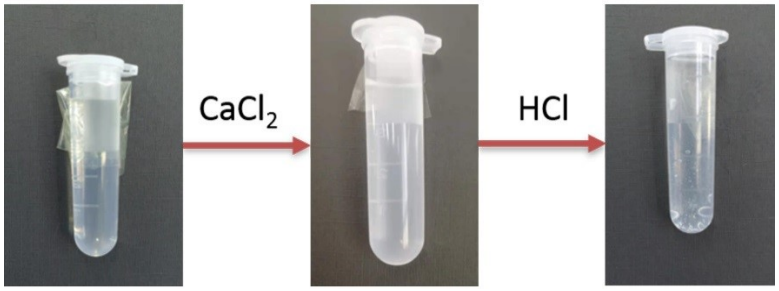

Fig. S13 Identification of carbonate in the products.

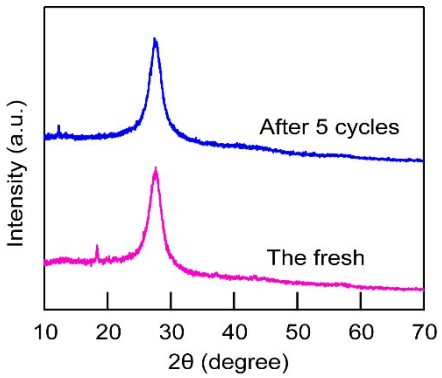

Fig. S14 XRD patterns of the fresh C_3N_4/r-Ti_3C_2 QDs-2 and after the fifth cycle of test.

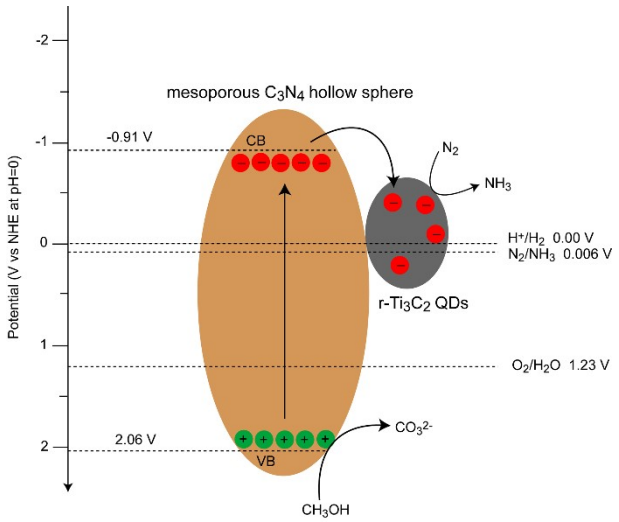

Fig. S15 Band energy diagram of the C_3N_4/r-Ti_3C_2 QDs Schottky junction.

Table S1 Comparison of different reported photocatalysts for photocatalytic N_2 fixation.

Photocatalysts	Experimental conditions	NH_3 production rate (μmol h^{-1} g^{-1}_{cat})	Test methods	Ref.
Fe-EDTA-C_3N_4	RT; visible light; methanol	50	Nessler's reagent	1
Hollow porous prismatic C_3N_4 with NVs	RT; visible light; methanol	118	Nessler's reagent	2
Au/TiO_2-OVs	RT; visible light; methanol	78.6	Indophenol blue	3
Fe(III)-C_3N4	RT; visible light	48.7	Nessler's reagent	4
BiOBr-001-OVs	RT; visible light	104.2	Indophenol blue	5
Bio-carbon-doped C_3N_4	RT; visible light; methanol	167.35	Nessler's reagent	6
MXene/TiO_2/Co	RT; UV-visible light	110	Nessler's reagent	7
TiO_2-250-OVs	RT; white light; methanol	116	Nessler's reagent	8
Fe-TiO_2/Au	RT; visible light	22.4	Indophenol blue	9
C_3N_4/r-Ti_3C_2 QDs	RT; white light/visible light; methanol	328.9/197.8	Nessler's reagent	This work

RT, room temperature; NVs, nitrogen vacancies; OVs, oxygen vacancies

Table S2 AQEs for N_2 photofixation in recent works

Photocatalyst	AQE	Reference
Au/hollow mesoporous C_3N_4 spheres with NVs	0.64% at 550 nm	10
Fe_2O_3 loaded porous g-C_3N_4	0.096% at 365 nm	11
$AgInS_2$/Ti_3C_2 Z-scheme heterojunction	0.07% at 420 nm	12
Cu-doped TiO_2	0.23% at 420 nm	13
Layered reduced Ti_3C_2/Au	0.697% at 520 nm	14
MXene-derived TiO_2@C@g-C_3N_4	0.14% at 420 nm	15
Nitrogen defective C_3N_4/BiO quantum dots	0.53% at 400 nm	16
$Ti_3C_2T_x$/TiO_2 calcined at 400 ^oC	0.05% at 630 nm,	17
F modified TiO_2 with OVs	0.38% at 420 nm	18
Bi_2WO_6 with OVs	0.04% at 420 nm	19
MoO_{3-x} nanosheets	0.31% at 808 nm	20
C_3N_4/r-Ti_3C_2 QDs	0.92% at 380 nm	This work

AQE, apparent quantum efficiency; NVs, nitrogen vacancies; OVs, oxygen vacancies.

References

1 C. K. Yao, R. Wang, Z. S. Wang, H. Lei, X. P. Dong and C. Z. He,*J. Mater. Chem. A*, 2019, **7**, 27547.

2 T. Huang, S. G. Pan, L. L. Shi, A. P. Yu, X. Wang and Y. S. Fu, *Nanoscale*, 2020, **12**, 1833.

3 J. H. Yang, Y. Z. Guo, R. B. Jiang, F. Qin, H. Zhang, W. Z. Lu, J. F. Wang and J. C. Yu, *J. Am. Chem. Soc.*, 2018, **140**, 8497.

4 H. Zeng, L. L. Liu, D. T. Zhang, Y. Wang, Z. H. Li, C. Liu, L. Zhang and X. Q. Cui, *Mater. Chem. Phys.*, 2021, **258**, 123830.

5 H. Li, J. Shang, Z. H. Ai and L. Z. Zhang, *J. Am. Chem. Soc.*, 2015, **137**, 6393.

6 Z. Tang, L. J. Xiong, X. Y. Zhang, J. Y. Shen, A. W. Sun, X. Y. Lin and Y. Yang, *Small*, 2021, 2105217.

7 W. G. Gao, X. M. Li, S. J. Luo, Z. L. Luo, X. Zhang, R. Huang and M. Luo, *J. Colloid Interface Sci.*, 2021, **585**, 20-29.

8 Q. Y. Liu, H. D. Wang, R. Tang, Q. Cheng and Y. J. Yuan, *ACS Appl. Nano Mater.*, 2021, **4**, 8674.

9 J. H. Yang, H. Y. Bai, Y. Z. Guo, H. Zhang, R. B. Jiang, B. C. Yang, J. F. Wang and J. C. Yu, *Angew. Chem. Int. Ed.*, 2021, **60**, 927.

10 Y. Z. Guo, J. H. Yang, D. H. Wu, H. Y. Bai, Z. Yang, J. F. Wang and B. C. Yang, *J. Mater. Chem. A,* 2020, **8**, 16218.

11 S. Z. Liu, S. B. Wang, Y. Jiang, Z. Q. Zhao, G. Y. Jiang and Z. Y. Sun, *Chem. Eng. J.*, 2019, **373**, 572.

12 J. Z. Qin, X. Hu, X. Y. Li, Z. F. Yin, B. J. Liu and K. Lam, *Nano Energy,* 2019, **61**, 27.

13 Y. X. Zhao, Y. F. Zhao, R. Shi, B. Wang, G. I. N. Waterhouse, L. Z. Wu, C. H. Tung and T. R. Zhang, *Adv. Mater.,* 2019, **31**, 1806482.

14 B. B. Chang, Y. Z. Guo, D. H. Wu, L. Li, B. C. Yang and J. F. Wang, *Chem. Sci.*, 2021, 12, 11213.

15 Q. X. Liu, L. H. Ai and J. Jiang, *J. Mater. Chem. A*, 2018, **6**, 4102.

16 C. Liang, H. Y. Niu, H. Guo, C. G. Niu, Y. Y. Yang, H. Y. Liu, W. W. Tang and H. P. Feng, *Chem. Eng. J.,* 2021, **406**, 12868.

17 T. T. Hou, Q. Li, Y. D. Zhang, W. K. Zhu, K. F. Yu, S. M. Wang, Q. Xu, S. Q. Liang and L. B. Wang, *Appl. Catal. B: Environ.,* 2020, **273**, 119072.

18 R. Q. Guan, D. D. Wang, Y. J. Zhang, C. Liu, W. Xu, J. O. Wang, Z. Zhao, M. Feng, Q. K. Shang and Z. C. Sun, *Appl. Catal. B: Environ.,* 2021, **282**, 119580.

19 T. Y. Wang, C. T. Feng, J. Q. Liu, D. J. Wang, H. M. Hu, J. Hu, Z. Chen and G. L. Xue, *Chem. Eng. J.,* 2021, **414**, 128827.

20 H. Y. Wu, X. Li, Y. Cheng, Y. H. Xiao, R. F. Li, Q. P. Wu, H. Lin, J. Xu, G. Q. Wang, C. Lin, X. Y. Chen and Y. S. Wang, *J. Mater. Chem. A,* 2020, **8**, 2827.